Mössbauer study of nanostructured iron fluoride powders

2000 J. Phys.: Condens. Matter 12 9497

(http://iopscience.iop.org/0953-8984/12/45/311)

J. Phys.: Condens. Matter **12** (2000) 9497–9509. Printed in the UK PII: S0953-8984(00)14999-9

Mössbauer study of nanostructured iron fluoride powders

H Guérault, M Tamine and J M Grenèche

Laboratoire de Physique de l'Etat Condensé, UMR CNRS 6087, Université du Maine, Faculté des Sciences, 72085 Le Mans Cedex 9, France

Received 22 June 2000, in final form 23 August 2000

Abstract. Nanostructured iron fluoride powders were prepared using the grinding route for different times and different intensities. Their structural, microstructural and magnetic properties are investigated by means of both transmission Mössbauer spectrometry as a function of temperature and in-field ^{57}Fe Mössbauer spectrometry. We report a fitting procedure which successfully describes the zero-field Mössbauer spectra recorded at different temperatures. It allows us to describe the powders as crystalline grains and grain boundaries which behave as antiferromagnets and speromagnets, respectively. Such arrangements are confirmed by in-field Mössbauer spectrometry. According to x-ray diffraction data, the size of grains and the thickness of grain boundaries are found to be strongly dependent on the grinding conditions. The occurrence of superparamagnetic effects at high temperature gives clear evidence for the role of grain boundaries in the magnetic coupling of crystalline grains.

1. Introduction

During the last decade, great attention has been devoted to both the high-energy ball grinding method and milled powders. Indeed, this route permits the preparation of the so called nanostructured materials, which display novel or even outstanding properties or combination of properties [1–3]. The modelling and predictions of these properties require an excellent knowledge of both the structure and the microstructure of the material. It is important to emphasize that the mechanical grinding process applied to crystalline compounds favours either the reduction of microcrystalline grains to grains composed of nanocrystalline structural domains, with or without structural transformation within the grains, or the synthesis of amorphous fine powders. The basic mechanism of ball grinding can be thus described as a succession of fracture and welding stages which occur during shocks and frictions, giving rise to an intimate reorganization at the mesoscopic scale. Consequently, the nanostructured powders obtained by such a route consist of particles composed of nanometre size crystalline grains linked to each other through grain boundaries: they behave as heterogeneous and partially disordered systems with a significant fraction of atoms expected to reside in defect environments (grain boundaries, surfaces) [1, 4, 5]. Their structural characterization requires *a priori* the use of diffraction techniques combined with local probe ones.

To model the microstructure of ball milled powders and to analyse the influence of the grinding conditions on the structure and on the thickness of grain boundaries, we selected ferric fluorides, which display several advantages. Indeed, FeF_3 exhibits a polymorphism with three different crystalline phases and two amorphous varieties [6], the structures of which result from ordered and disordered packing of corner-sharing octahedral units respectively. Those rather different cationic topologies originate collinear and non-collinear magnetic arrangements in

0953-8984/00/459497+13$30.00

conjunction with the antiferromagnetic nature of the superexchange interactions [6, 7] and iron fluoride is therefore considered as 'excellent simple model systems' to illustrate the concept of topological magnetic frustration. The more stable crystalline FeF_3, which is the rhombohedral phase (r-FeF_3; SG: $R-3c$) behaves as a weak ferromagnet structure below $T_N = 363$ K, while a strong reduction of the Néel point is observed for the other two phases (hexagonal tungsten bronze HTB-FeF_3: $T_N = 110$ K and pyrochlore pyr-FeF_3: $T_N = 22$ K), due to the frustrated cationic topology. The amorphous varieties (a-FeF_3) are speromagnets below the freezing temperature ranging from 30 to 40 K [8, 9]. Moreover, both the hyperfine field and the magnetic moment decrease with increasing number of frustrated interactions whereas the isomer shift is rather insensitive. Taking those features into account, one expects to distinguish easily crystalline grains and grain boundaries because they may exhibit different magnetic arrangements.

In addition, the nature of the microstructure of these two-phase materials (grain size and grain boundary thickness) favours the occurrence of a total magnetic behaviour that is strongly temperature dependent and of magnetic thermal fluctuations at high temperature. Indeed, the magnetic length range characterizing the superexchange interactions in the ionic systems is estimated at about 1 nm, which is much smaller than that of metallic systems. Consequently the presence of grain boundaries in ionic nanostructured powders originates high temperature dynamic effects: the larger the grain boundaries, the higher the thermal fluctuation effects.

^{57}Fe Mössbauer spectrometry (MS) is a selective nuclear technique which is particularly suitable to investigate both the structural and magnetic behaviour of Fe-containing nanostructured powders [10]. Indeed, it is able to distinguish the different iron species according to their atomic arrangement, i.e. crystalline grains and disordered grain boundaries, and to estimate the content of both components. In addition, the characteristic time measurement of ^{57}Fe MS (10^{-8} s) offers a high sensitivity to superparamagnetic effects [11, 12], which is well adapted to ferromagnetic and ferrimagnetic nanophase systems and remains well adapted to such antiferromagnetic systems despite the smaller relaxation time.

r-FeF_3 powder was ball milled for several durations under different grinding intensities. Different nanostructured fluoride powders were obtained and then studied by different techniques with complementary spatial and time scales. The aim of the present paper is the modelling of the microstructural and magnetic properties of these powders, essentially based on MS. This approach was successfully developed combining measurements performed at different temperatures and under applied field, and carried out on powders milled for different times and different grinding intensities.

2. Experimental section

High-energy ball grinding was carried out using a commercial Fritsch Pulverisette 7 planetary ball-mill to induce particle size evolution of microcrystalline grains of rhombohedral phase of FeF_3. Four zircon balls were used in each zircon vial with a powder-to-ball weight ratio of 1/30. Owing to the high hygroscopic behaviour of fluorides and the high surface reactivity of the final powders, they were milled and conditioned in a dried atmosphere (Ar) to prevent any moisture.

The present study concerns FeF_3 powders milled for from 15 min to 16 h at intensity $I = 6$ (vial rotation speed of 800 tr min^{-1}) and 20 h at $I = 10$ (1400 tr min^{-1}). Zero-field and in-field ^{57}Fe Mössbauer spectra were recorded at different temperatures cooling the sample in a bath cryostat or a cryomagnetic device where the external field (6 T) is oriented parallel to the γ-beam. The measurements are made in standard transmission geometry, using a ^{57}Co source in an Rh matrix. The sample consists in a 5 mg Fe cm^{-2} milled FeF_3 powder mixed

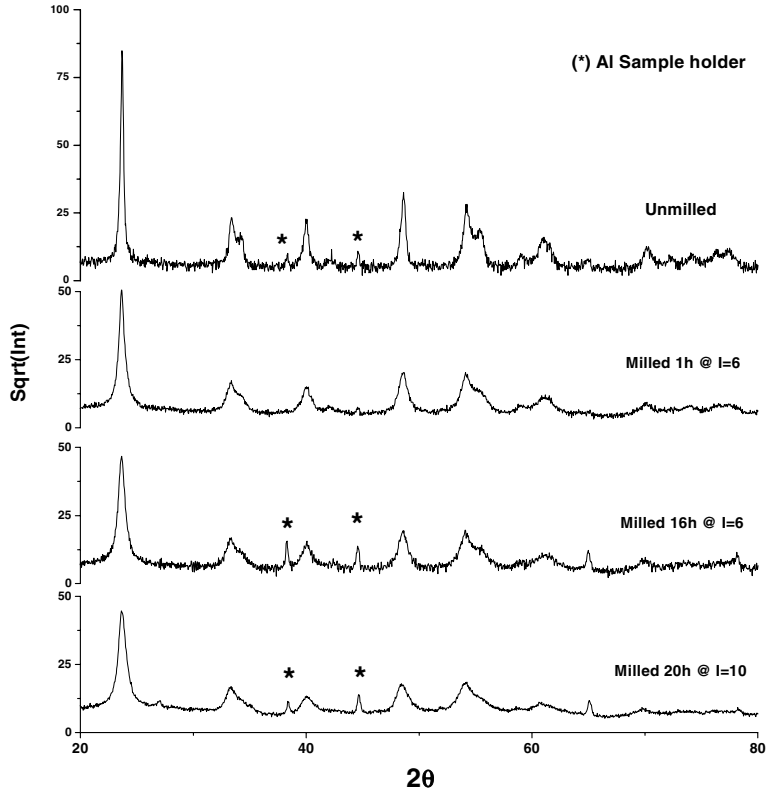

Figure 1. XRD patterns of iron fluoride milled powders.

with dry AlF_3 to optimize the counting rate and to prevent hydrolysis. The isomer shift values are quoted relative to that of α-Fe at room temperature and the zero-field and in-field spectra were fitted using the MOSFIT and MOSHEX programs, respectively [13].

3. X-ray diffraction (XRD) study: results and discussion

X-ray patterns were taken on the fluoride powders milled for different durations under different grinding intensities, using a Phillips X'pert diffractometer (with monochromatized Cu Kα radiation; $\lambda = 1.540\,56$ Å). The different milled powders were conditioned under a controlled atmosphere in a special sample chamber with a circular slot recovered with a 8 μm polyimide film (Kapton) to minimize the background scattering level [14]. A selection of x-ray diffraction patterns is reported in figure 1. One observes clearly a broadening of Bragg peaks when the grinding time increases. Consequently, the x-ray patterns were analysed by the RIETQUAN procedure [15], which is based on the Rietveld method combined with a Fourier analysis, well adapted for broadened diffraction peaks. This method thus allows the refinement of the structural and microstructural parameters, the lattice parameters and the size and the microstrains of crystalline domains.

For the powders milled with intensity 6, the x-ray patterns are well reproduced by means of a single crystalline component, which corresponds to r-FeF_3. One concludes that there is no structural transformation of the crystalline phase during the mechanical process. As

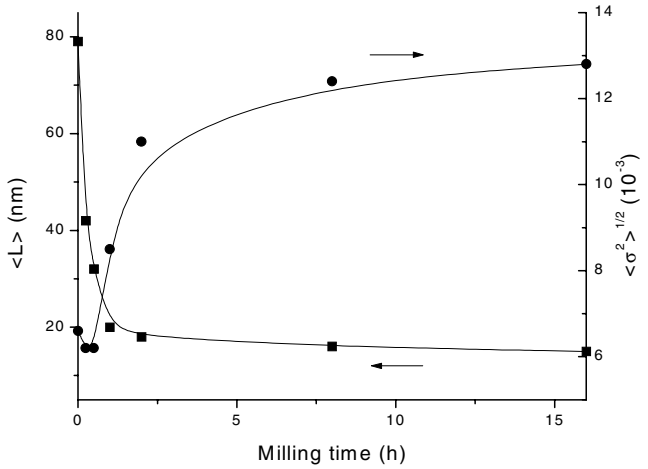

Figure 2. Mean size $\langle L \rangle$ and microdeformation $\langle \sigma^2 \rangle^{1/2}$ evolution with grinding duration ($I = 6$).

Table 1. Structural and microstructural data of iron fluoride milled powders.

	Crystalline grains						Grain boundaries	
	a (Å)	c (Å)	x_f	$\langle L \rangle$ (nm)	$\langle \sigma^2 \rangle^{1/2}$ (nm)	%	$\langle e \rangle$ (nm)	%
Unmilled	5.230 (1)	13.285 (1)	0.581 (2)	80 (5)	6.6 (0.3) $\times 10^{-3}$	100	—	—
$I = 6$, 16 h	5.221 (2)	13.330 (2)	0.586 (4)	16 (2)	12.9 (0.3) $\times 10^{-3}$	85 (5)	1 (0.5)	15 (5)
$I = 10$, 20 h	5.200 (5)	13.276 (5)	0.583 (6)	16 (2)	13.8 (0.3) $\times 10^{-3}$	57 (5)	4 (0.5)	43 (5)

shown in figure 2, the grain size $\langle L \rangle$ rapidly decreases down to 20 nm after small grinding times, while the microstrains increase; then, for long grinding times, size and microstrains are stabilized. When the grinding intensity is higher, the single component fitting procedure is no longer consistent, especially for the reproduction of the bottom of the peaks. Thus, the refinement of x-ray patterns requires the use of a second component characterized by a lack of long range order as encountered in an amorphous phase: it is thus attributed to the grain boundaries. This second fitting procedure was then applied to different patterns and the refinement allows the atomic proportions of both the grain boundary and the crystalline grain to be estimated [14]. Consequently, the average thickness of grain boundaries $\langle e \rangle$ is established assuming a core–shell model. The main structural and microstructural data are listed in table 1. One notes that the lattice parameters are close to those of the unmilled rhombohedral phase and remain independent of the grinding conditions. Details of the x-ray analysis are reported in [14] and will be published elsewhere.

4. ^{57}Fe Mössbauer spectrometry: results and discussion

Some significant Mössbauer spectra are illustrated in figures 3 and 4 which allow us to compare the hyperfine structure at different temperatures (300, 77 and 4.2 K respectively) for different grinding times and for two different grinding intensities. Thus, room temperature spectra exhibit a strong evolution with grinding time: one observes a broadening of the magnetic lines, a decrease of their intensity and at the same time a progressive appearance of a broad single

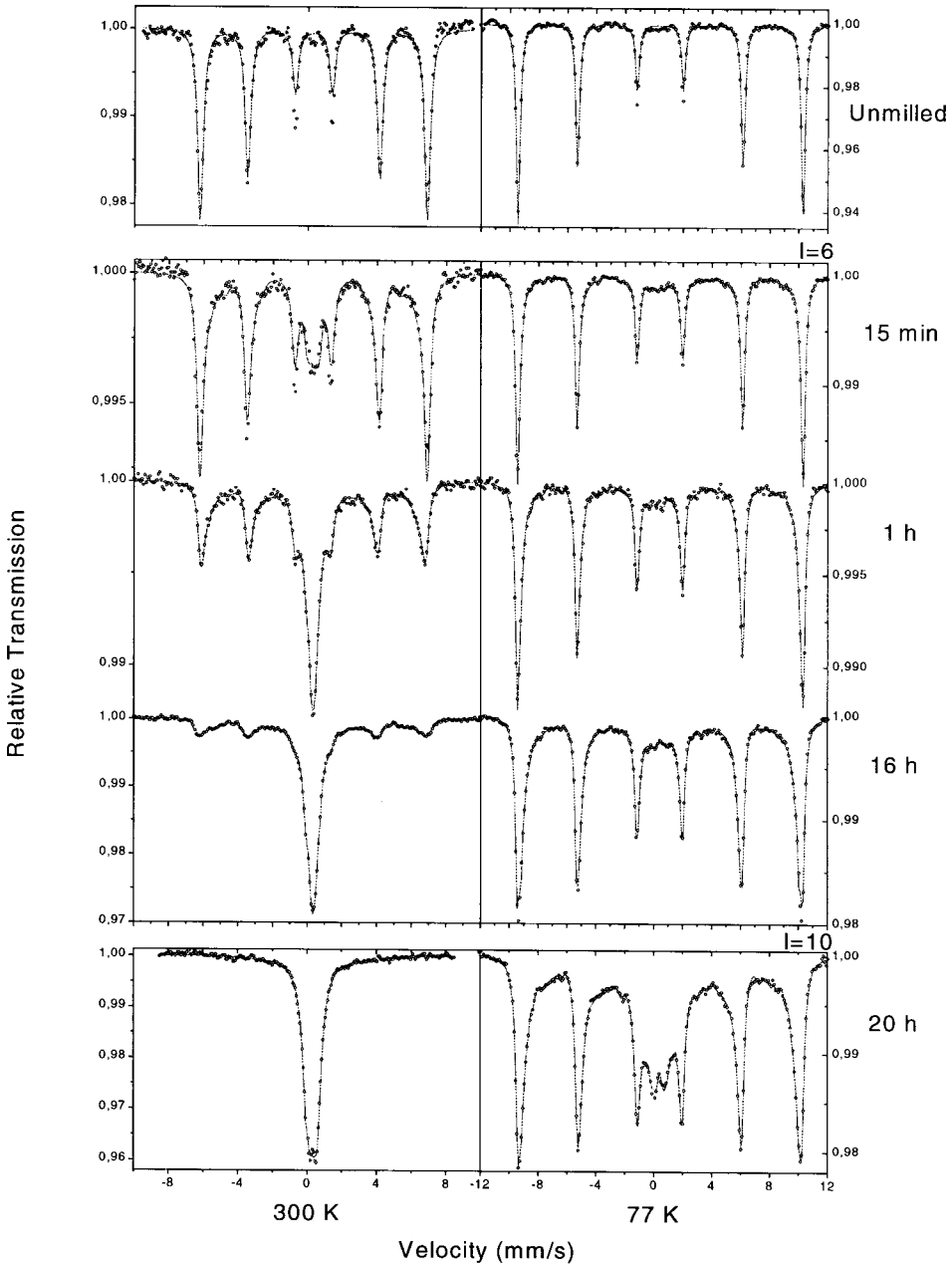

Figure 3. 300 K and 77 K Mössbauer spectra of iron fluoride milled powders.

line in the low velocity range, which becomes the prevailing contribution to the absorption for a 16 h grinding at intensity 6. Likewise, higher grinding intensity leads to similar effects but one finally observes the total disappearance of the magnetic lines. At 77 K, the evolution of the hyperfine structure differs from that at 300 K: an increasing asymmetric broadening of the magnetic lines is observed with increasing grinding time, giving rise to the emergence of a low

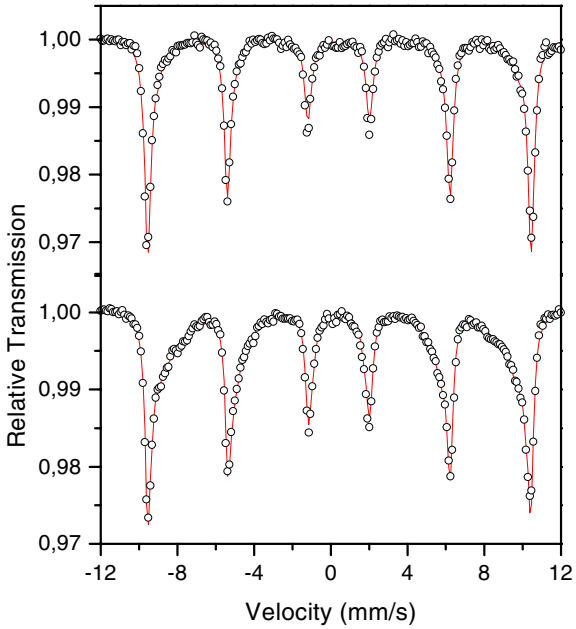

Figure 4. 4.2 K Mössbauer spectra of iron fluoride milled powders (top, 16 h, $I = 6$; bottom, 20 h, $I = 10$).

intensity quadrupolar central doublet. In addition, the spectra obtained in the highest grinding intensity powders are characterized by a progressive lowering of the base line which leads to a well defined quadrupolar doublet. Finally, at 4.2 K, the hyperfine structures of the milled powder spectra are close to that of the unmilled powder spectrum. However, the increasing asymmetric broadening of the magnetic lines with both grinding time and grinding intensity, indicates an hyperfine field reduction for a significant part of iron atoms. One can *a priori* suggest the occurrence of atomic disorder originating from the grinding effect.

As a first fitting approach, we have considered a discrete hyperfine field distribution with a common isomer shift value, taking the symmetry of spectra into account (figure 5). The spectra are quite well reproduced and some first conclusions can be drawn at this stage.

(i) The refined value of the isomer shift is similar to that characteristic of the unmilled r-FeF_3 phase, whatever the grinding time is. Such a feature indicates that all the iron atoms are located in corner-sharing fluorine octahedral units, that is consistent with x-ray diffraction conclusions.

(ii) The highest hyperfine field value is found to be identical to that of the initial crystalline r-FeF_3 phase, corresponding to a pseudo-cubic packing of corner-sharing octahedral units: this suggests that the remaining crystalline contribution exhibits the same structure as in the initial phase.

(iii) The low-temperature hyperfine field reduction resulting from the asymmetric broadening of the magnetic lines at 4.2 K can be attributed to the presence of corner-sharing octahedral units for which the arrangement favours antiferromagnetic frustrated interactions. By comparing the present values to those established for both crystalline and amorphous ferric fluoride species, a topology with triangular packing of octahedral units has to be present in the disordered grain boundaries which connect crystalline ordered grains. It is important to emphasize that one can roughly estimate the proportion of resonant nuclei located in

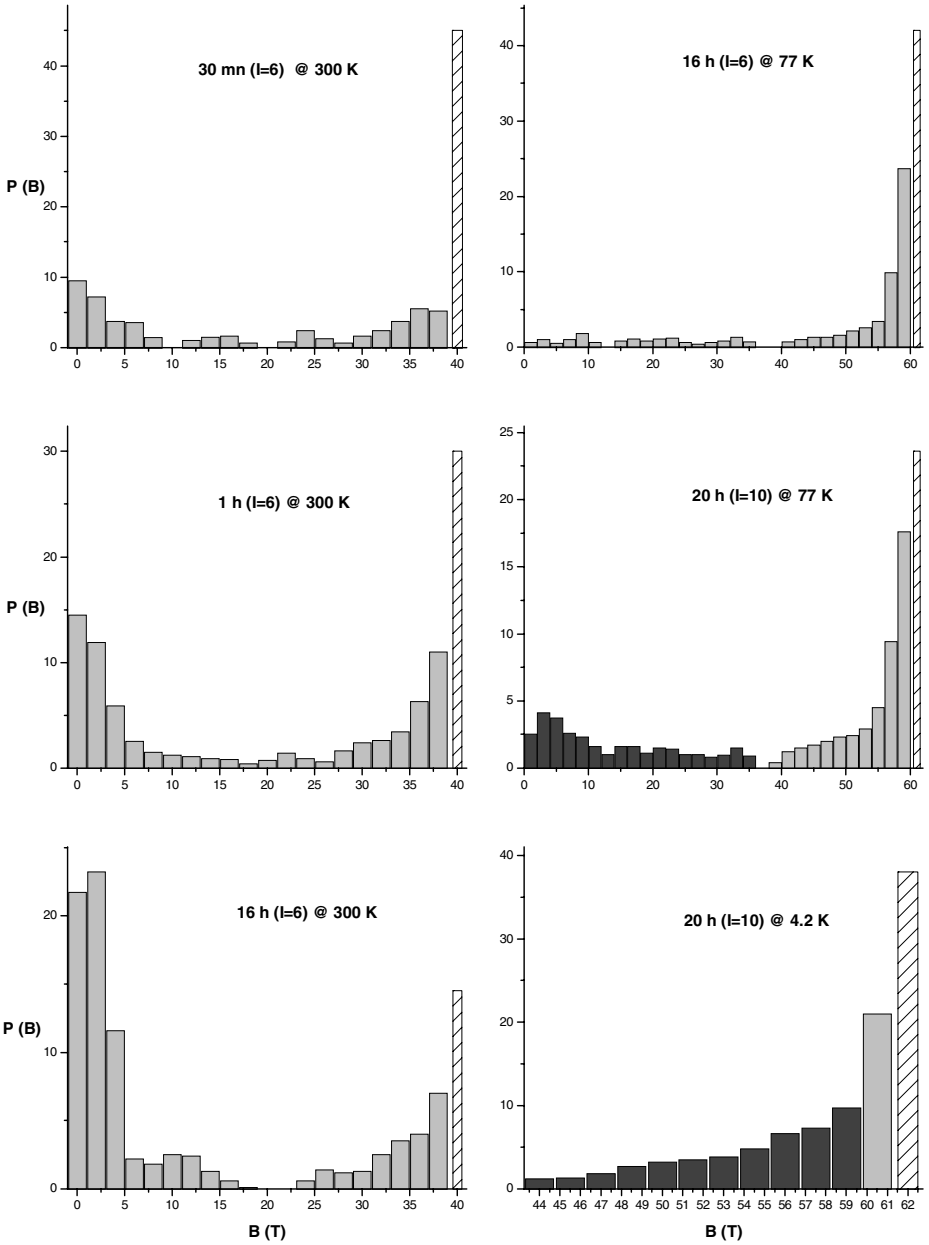

Figure 5. Field distributions for different milling durations and intensities. The dark bars represent the hyperfine field distribution in GB at 77 K and 4.2 K. The hatched bars represent the r-FeF_3 crystalline contribution in the distributions.

both crystalline grains and grain boundaries, assuming the same recoilless factor value for these two contributions. The proportion of Fe present within the grain boundaries is found to be approximately 15 at.% for the 16 h grinding time at intensity 6 and significantly increases up to 42% for the 20 h grinding time at intensity 10, while that of atoms located

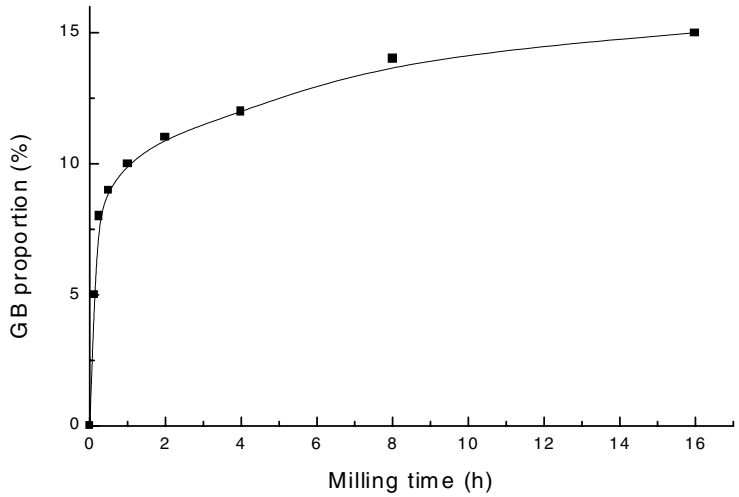

Figure 6. Grain boundary proportions estimated at 77 K in milled FeF_3 ($I = 6$) versus milling time.

in the crystalline grains decreases, in agreement with x-ray diffraction results.

(iv) The broadened quadrupolar doublet contribution observed at 77 K is strictly similar to the grain boundary proportion previously estimated. Thus the topological reorganization at grain boundaries toward frustrating topologies induces a magnetic transition to a paramagnetic state at a temperature lower than that characteristic of the grains.

(v) The broad single line absorption observed at 300 K is larger than the paramagnetic contribution of the grain boundaries observed at low temperature. The recoilless factors characteristic of the crystalline phase and of the grain boundaries cannot explain such a difference and the presence of dynamic phenomena in the crystalline grains has therefore to be invoked to explain the high paramagnetic proportion. Indeed, the crystalline grains can display a high temperature superparamagnetic behaviour because the paramagnetic grain boundaries originate an assembly of non-interacting magnetic grains. The presence of superparamagnetic effects was easily checked by recording a spectrum at room temperature on a milled powder subjected to a small magnetic field (0.1 T). A significant symmetric broadening of the central line is noticed, indicating a reduction of the magnetic fluctuations in the crystalline grains. Thus, the central absorption line proceeds from the superimposition of a paramagnetic contribution assigned to the grain boundaries and a superparamagnetic contribution resulting from the crystalline grains.

Taking into account the previous features, one can establish a more appropriate fitting procedure, in which the two components assigned to the crystalline grains and the grain boundaries are independently modelled. The main objective is to follow the crystalline grain and the grain boundary proportions, their respective hyperfine parameters and their dependence on temperature. The results are now discussed according to the following pertinent parameters.

4.1. Grinding time effect

The crystalline grain and the grain boundary proportions estimated from spectra recorded at 77 K are represented versus grinding time for powders milled at intensity 6 in figure 6. It clearly

evidences a microstructural evolution mainly concentrated in the first two grinding hours, in agreement with the proportion and grain size evolution observed by XRD. The nanometre size of the crystalline grains is confirmed by MS by the appearance of magnetization fluctuations at high temperature. Consequently, the complex hyperfine structure of the crystalline grains at room temperature results from the superimposition of magnetic and superparamagnetic contributions, in agreement with magnetic measurements [14]: that suggests a grain size distribution the width of which decreases with increasing grinding time.

At low temperature, the asymmetric broadening of the magnetic lines which is attributed to the grain boundary contribution, is well reproduced by an hyperfine field distribution. Its main characteristics (isomer shift and mean hyperfine field values) are similar to those of the amorphous phases [8, 9] (table 2). Thus, the magnetic arrangement in those disordered zones is by analogy assumed to be speromagnetic, as will be confirmed below.

The microstructure of iron fluoride nanostructured powders can therefore be described by an ordered (grains) and a random (grain boundaries) packing of corner-sharing octahedral units. However, a precise refinement of the external magnetic lines at 4.2 K evidences the necessity of two components to be used and a third magnetic environment can finally be distinguished by MS. The first sextet presents the same hyperfine parameters as those of the unmilled powder (r-FeF_3). The second one presents the same isomer shift value, but a hyperfine field reduction of 1 T. This second ordered component is attributed to the periphery of the crystalline grains, magnetically perturbed by the magnetic disorder of the grain boundaries. According to the crystalline size obtained by XRD, the thickness of this perturbed magnetic zone is estimated at 1 to 2 octahedral units ($\sim$0.5–1 nm); such a thickness is of the same order as the superexchange interaction length.

4.2. Grinding intensity effect

The fitting procedure previously described remains available for powders milled at higher intensity and the three magnetic environments at low temperature are still (and even better) observed. However, the microstructure differs in the higher proportion of resonant nuclei located in grain boundaries, the thickness of which have notably increased (3–4 nm), whereas the mean grain size has not changed, according to the XRD results. The increase of the interparticle distance to values higher than the super-exchange interaction length (1 nm) favours the magnetic decoupling of the crystalline grains, that explains the disappearance of the magnetic lines at high temperature.

4.3. Temperature effect

Figure 7 shows the hyperfine field versus temperature for the powder milled at intensity 10 compared to that of unmilled powder. The decomposition into two components associated with different structural environments for the milled powders is also represented. In the case of milled powders, three temperature ranges can be distinguished.

(i) In the low temperature range, the two phases are magnetically ordered but display two different magnetic structures: antiferromagnetic in the crystalline grains and speromagnetic in the grain boundaries. The hyperfine field values of each component well agree with those of the rhombohedral and of the amorphous phases, respectively.

(ii) With increasing temperature, the grain boundary moments progressively transit to a paramagnetic state, with defrosting temperatures ranged between 100 and 200 K. This large temperature distribution is attributed to both the grain size distribution and the heterogeneous thickness of the grain boundaries. In addition, dynamic phenomena can

Table 2. Structural, magnetic and hyperfine characteristics of crystalline, nanostructured and amorphous iron fluorides.

		Crystalline phases			Nanostructured powders[a]		Amorphous phases	
Characteristics		r-FeF_3	HTB-FeF_3	Pyr-FeF_3	Grains	Grain boundaries	a-FeF_3	a-FeF_3, xHF
Structural	Space group	$R-3c$	$P6/mmm$	$Fd3m$	$R-3c$	Disordered	Disordered	Disordered
	Cationic network	Cubic	Hexagonal & triangular	Triangular	Cubic	Random	Random	Random
Magnetic	Spin structure	Antiferro	Triangular	Triangular	Antiferro	Speromagnet	Speromagnet	Speromagnet
	Transition	$T_N = 363$ K	$T_N = 97$ K	$T_N = 20$ K	$\langle T_B \rangle = 250$ K	$100 < T_G < 200$ K	$T_G = 36$ K	$T_G = 36$ K
Hyperfine	IS (mm s^{-1})[b]	0.49	0.47	0.48	0.485	0.45	0.46	0.46
	B (T)[c]	61.8	56	52.3	61.5	54.5	56	55

[a] Obtained by grinding r-FeF_3 powders.
[b] At 300 K relative to α-Fe.
[c] At 4.2 K

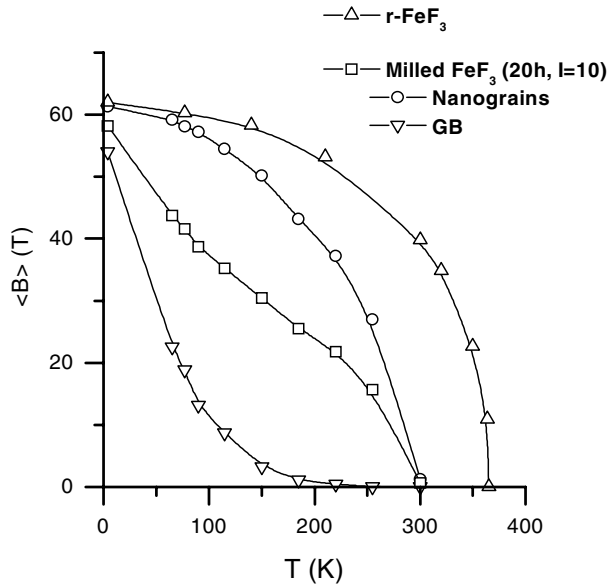

Figure 7. Mean hyperfine field values versus temperature in massive r-FeF_3 (△) and nanostructured FeF_3 (average field □, crystalline grains ○ and grain boundaries ▽).

occur in the grains. In contrast with the topological analogy between amorphous phases and the grain boundaries of milled powders giving rise to same hyperfine characteristics, one does remark that the magnetic freezing temperatures of the grain boundaries are found higher than those of the amorphous phases (100–200 K and 30–40 K, respectively). Such a difference partly originates from the structural disorder of the grain boundaries which can differ from that of the amorphous phases. The polarization of the grain boundaries by the crystalline grain also enhances their magnetic ordering temperature.

(iii) At high temperature, the grain boundaries become paramagnetic and the single domain grains have a superparamagnetic behaviour. Indeed, one expects a progressive magnetic decoupling between grains as effective as the thickness of the grain boundaries is large, leading to an assembly of non-interacting antiferromagnetic particles. The distribution of grain size and of the thickness of grain boundaries originates a distribution of blocking temperature ranging from 200 up to 360 K (corresponding to the Néel temperature of r-ReF_3), that is confirmed by static magnetic measurements [14].

4.4. Applied field effect

An in-field Mössbauer spectrum was recorded on the 20 h intensity 10 milled powders subjected to a 6 T field oriented parallel to the γ-beam (figure 8), in order to check the speromagnetic arrangement in the grain boundaries, as previously mentioned. The spectrum is fitted by means of two components associated with two different magnetic arrangements: (i) a sextet with sharp lines, the intensities of which are 3:4:1:1:4:3, typically observed for an antiferromagnetic structure and (ii) a sextet with broadened lines with a particular profile, corresponding to a speromagnetic system [7–9, 16, 17]. These two components are assigned to the antiferromagnetic crystalline grains, and to the grain boundaries, respectively. The fitting procedure unambiguously leads to a set of refined hyperfine parameters which are

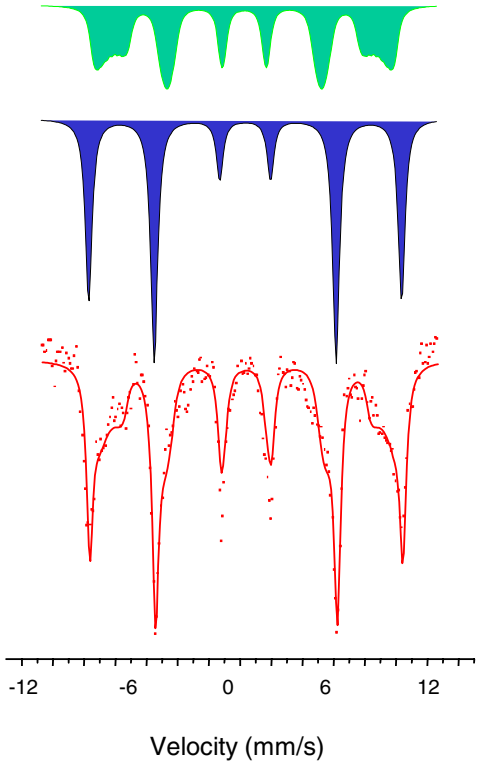

Figure 8. In-field Mössbauer spectra of 20 h ($I = 10$) milled FeF_3 powder (bottom) and its decomposition (top, speromagnetic, and middle, antiferromagnetic components attributed to grain boundaries and crystalline grains, respectively—see text).

consistent with those of the rhombohedral r-FeF_3 phase and of the amorphous phases [7–9]. In addition, it is important to note that the phase proportions estimated from this refinement are similar to those obtained from the zero-field Mössbauer spectra and x-ray diffraction. Such a quantitative agreement fairly well supports the fitting procedure previously developed and applied to describe the series of zero-field Mössbauer spectra.

5. Conclusions

The present study illustrates first that a single local probe technique such as Mössbauer spectrometry, is suitable to get relevant structural, microstructural and magnetic data on nanostructured powders prepared by mechanical grinding, provided that (i) the unmilled powders are well characterized, (ii) various experimental conditions have to be used (temperature, external field, grinding intensity and grinding time) and (iii) the hyperfine structures have to be carefully modelled. The fitting method thus requires analysing the spectra individually in a first stage, and then the series of spectra mutually. It also reveals that this ferric fluoride is confirmed to be an excellent model system because the topology based on different octahedral unit arrangements originates a variety of magnetic structures. Finally, this study clearly confirms that the grain boundaries have to be taken into account because they play an important role in the magnetic coupling of crystalline grains.

References

[1] Gleiter H 1989 *Prog. Mater. Sci.* **33** 223
[2] Hernando A, Vasquez M and Paramo D 1998 *Mater. Sci. Forum* **269–272** 1033
[3] Edelstein A S and Cammarata R C 1996 *Nanomaterials: Synthesis, Properties and Applications* (Bristol: Institute of Physics)
[4] Guérault H and Grenèche J M 2000 *J. Phys.: Condens. Matter* **12** 4791
[5] Bureau B, Guérault H, Silly G, Buzaré J Y and Grenèche J M 1999 *J. Phys.: Condens. Matter* **11** L423
[6] Ferey F, Leblanc M, De Pape R and Pannetier J 1985 *Inorganic Solid Fluorides* ed Hagenmuller (New York: Academic) p 395
[7] Greneche J M and Varret F 1993 *Mössbauer Spectroscopy Applied to Magnetism and Materials Science* ed G Long and F Grandjean (New York: Plenum) p 161
[8] Ferey G, Varret F and Coey J M D 1979 *J. Phys. C: Solid State Phys.* **12** L531
[9] Grenèche J M, Le Bail A, Leblanc M, Mosset A, Varret F, Galy J and Ferey G 1988 *J. Phys. C: Solid State Phys.* **21** 1351
[10] Grenèche J M 1999 *Mater. Sci. Forum* **307** 159
[11] Dormann J L 1981 *Rev. Phys. Appl.* **16** 275
[12] Dormann J L, Fiorani D and Tronc E 1997 *Advances in Chemical Physics* vol 98, p 293
[13] Teillet J and Varret F *Mosfit and Moshex Programs* Université du Maine, unpublished
[14] Guérault H 2000 *Thesis* University of Le Mans
[15] Lutterotti L and Scardi P 1990 *J. Appl. Crystallogr.* **23** 246
[16] Chappert J, Teillet J and Varret F 1979 *J. Magn. Magn. Mater.* **11** 200
[17] Grenèche J M 1995 *Acta Phys. Slovaca* **45** 45